Journal of
MATERIALS RESEARCH

Superparamagnetic particles in ZSM-5–type ferrisilicates

A. López, F. J. Lázaro,[a] J. L. García-Palacios, and A. Larrea
Instituto de Ciencia de Materiales de Aragón (Universidad de Zaragoza-Consejo Superior de Investigaciones Científicas), 50015 Zaragoza, Spain

Q. A. Pankhurst
Department of Physics and Astronomy, University College London, London WC1E 6BT, United Kingdom

C. Martínez and A. Corma
Instituto de Tecnología Química (Consejo Superior de Investigaciones Científicas), 46022 Valencia, Spain

(Received 28 October 1996; accepted 23 January 1997)

As-synthesized, low iron content, ferrisilicates of ZSM-5-type contain well-separated Fe(III) ions in a tetrahedral environment and display paramagnetic behavior. After hydrothermal treatment, the iron ions are partially extracted from the framework, generating nanosize iron oxide or oxyhydroxide ferrimagnetic particles. This process has been studied by transmission electron microscopy (TEM), Mössbauer spectroscopy, magnetic ac susceptibility (χ_{ac}), and field dependent magnetization, on samples containing up to 6.7 wt.% Fe. The experiments evidence the growth of nonaggregated particles, with a typical size around 3 nm, presumably located at the surface of the ferrisilicate crystallites. From a thorough granulometric analysis involving TEM and χ_{ac} data, it is concluded that, in the range from 1.5 to 4.6 wt.% Fe, the particle size distributions are significantly independent of the iron content.

I. INTRODUCTION

The development of experimental techniques able to explore the structure of matter at the nanometric level has recently stimulated the research on the so-called nanostructured materials.[1] An interesting subclass are the nanodispersions, that is, particulate assemblies dilutely supported in a matrix, either solid or liquid. To this group belong, for example, the magnetic colloids,[2] dilute granular alloys,[3] and some catalysts.[4] The size of the nanometric entities contained in those materials strongly affects their properties and, since the presence of very small clusters or even isolated atoms also play a role in some cases, the knowledge, as complete as possible, of the size distribution is a matter of prime interest in their characterization.

In practice, conventional techniques, usually of diffraction type, which cover the upper nanometric range (dimensions greater than about 10 nm), fail in identifying species of the order of few lattice parameters, especially if they are diluted and randomly distributed in a matrix.[5] An example of such a difficult task appears in zeolite supported cluster assemblies, where not only the mere presence of the clusters but also their location with respect to the zeolite crystallites are important parameters in their characterization.[6] To get insight into this problem, and in addition to transmission electron microscopy (TEM) whose valuable contribution to explore the nanometric range is out of any discussion, other techniques like Mössbauer spectroscopy[7,8] or magnetic methods[9–11] are sometimes employed.

In this work, the above mentioned issues are addressed within an experimental study of ferrisilicates of ZSM-5 type. These materials receive great attention as catalysts and possess a porous crystalline structure.[12] The isomorphous reference material, silicalite, contains silicon atoms in a tetrahedral environment. While in ZSM-5, the silicon sites are partially occupied by aluminum, in the studied ferrisilicates the substituent atom is Fe(III). In these materials, like in other metallosilicates,[12] the catalytic activity is affected by hydrothermal treatments, due to the extraction of iron ions from framework sites leading to their aggregation into iron oxide or oxyhydroxide clusters in the cavities or at the crystallite surface.[8] Since the synthesis of these materials involves a hydrothermal treatment, the study of the effects of iron migration as a consequence of such treatments is of key interest.

In this paper, TEM, field dependent magnetization, temperature dependent ac initial susceptibility at various frequencies, and field and temperature dependent Mössbauer spectroscopy results, obtained from laboratory synthesized ferrisilicates, are presented. This is done with two objectives in mind: (i) to establish the extent

[a]Author to whom correspondence should be addressed.

to which magnetism may be used to characterize iron in framework positions and to monitor their migration induced by hydrothermal treatments, and (ii) to perform a granulometric analysis of a nanostructured assembly of nonaggregated particles with size distribution properties that might also be amenable to fundamental magnetic studies.

II. EXPERIMENTAL DETAILS

Fe-MFI[13] samples with different Si/Fe ratios were prepared by hydrothermal synthesis following the procedure described previously,[14] varying the composition of the gel. The synthesis mixture contained amorphous silica (AEROSIL 200, Degussa), tetrapropylammonium bromide, TPABr (98%, Aldrich), iron nitrate (97%, Probus), and sodium hydroxide (98%, Prolabo) in the following molar ratios: $TPABr/SiO_2 = 0.06$, $H_2O/SiO_2 = 44.33$, and $SiO_2/Na = 4.61$. The different Si/Fe ratios in the synthesis gel are given in Table I. Diluted sulfuric acid (95%, Probus, $H_2SO_4 : H_2O$ molar ratio of 1 : 4) was added to the synthesis gel to maintain a pH value of 12. Crystallization of the gels was carried out in PTFE-lined stainless steel stirred autoclaves at 150 °C. Hydrothermal treatments (100% steam at atmospheric pressure) were carried out at 1023 K for 3 h, with the exception of the sample of 4.6% Fe, which was obtained by steam calcination at 723 K for 3 h.

The samples differed in color depending on their Fe(III) concentration and on the thermal treatment (Table I). On the basis of Mössbauer results, Meagher *et al.*[8] concluded that a white color is a necessary but not sufficient condition for having all the iron in framework sites. All of our as-synthesized samples are white. Hydrothermal treatment produces colored samples for iron concentrations $\geqslant$ 1%, with the colors varying from off-white to brown, through several yellow intensities, with increasing iron content.

TEM experiments were performed in a JEOL 2000 FX II microscope operated at 200 kV (point to point resolution: 2.8 Å) and equipped with an Oxford/Link energy dispersive spectrometry (EDS) analytical system (resolution: 141 eV at 5.9 keV). To prepare specimens for TEM observations, samples were crushed in an agate mortar, dispersed in acetone, and placed onto a carbon reinforced lacey formvar microgrid.

Mössbauer spectra were recorded using a 50 mCi unpolarized ^{57}CoRh source of 14.4 keV ^{57}Fe γ-rays. Constant acceleration mode was used, with the source velocity following a triangular drive waveform. Spectra were recorded in a 576 channel multichannel analyzer, and were folded to remove baseline curvature. Calibration between channel and source velocity was with reference to an $\alpha-$Fe foil at room temperature. Low temperature spectra were recorded in a liquid helium bath cryostat, and applied field spectra were obtained using a 10 T superconducting magnet.

Dynamic ac susceptibility and field dependent magnetization measurements were performed in a SQUID magnetometer (Quantum Design) equipped with an ac option. The amplitude of the ac exciting field was 0.11 mT and the frequencies used were in the range 0.1 Hz–1000 Hz.

III. EXPERIMENTAL RESULTS

A. Transmission electron microscopy

For the microstructural studies, as-synthesized and hydrothermally treated samples with different Fe concentration were observed via TEM. EDS microanalysis of all these samples confirms the expected chemical composition, in particular the presence of iron. Typical micrographs are shown in Fig. 1. All the steamed samples of high Fe concentration (greater than 1%) display the presence of nonaggregated small particles with typical size around 3 nm, while the as-synthesized and the steamed ones of low Fe concentration (less than 1%) do not contain observable particles. In general it is not possible, from a transmission micrograph, to elucidate whether the particles are inside the ferrisilicate crystallites or at their surface. However, owing to their size, several times larger than the ferrisilicate cavities, and to the observation of some of them at the border of the crystallites [see in particular Fig. 1(c)] we infer that the surfaces are probably their preferential location. The particle size distributions obtained from a statistical analysis of the micrographs are shown in Fig. 2. As can

TABLE I. Description of the concentrations and colors of the samples used in this study.

Si/Fe in gel[a]	Wt. % Fe in sample	As-synthesized	Hydrothermally treated (750 °C)
300	0.4	white	white
100	1	white	off-white
60	1.6	white	yellow
35	2.8	white	brown
20	4.6	white	light brown[a]
15	6.7	white	brown

[a]Molar ratio.
[b]This sample was treated at 450 °C.

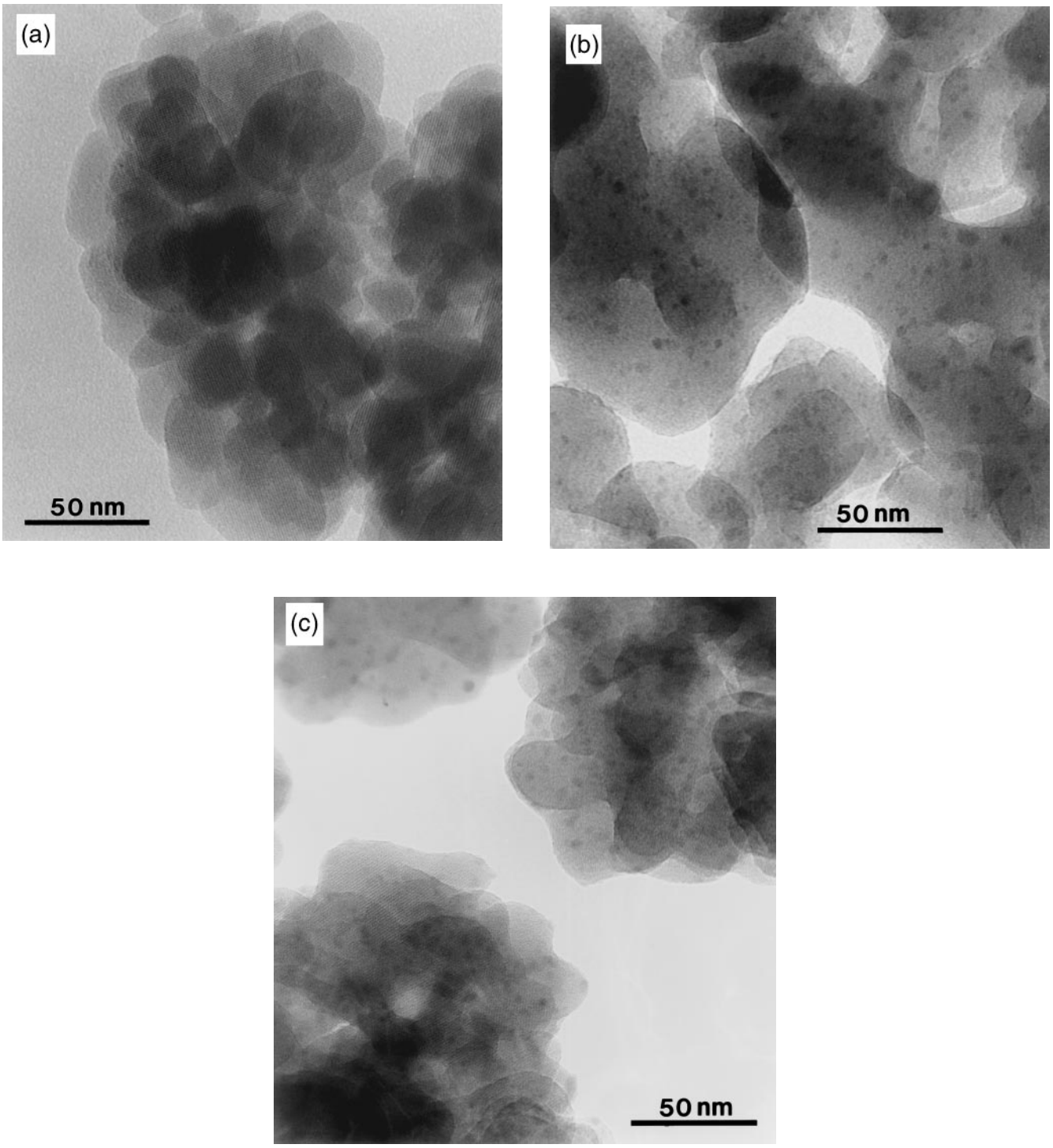

FIG. 1. TEM micrographs of (a) the as-synthesized sample with 4.6 wt.% Fe, (b) the steamed sample with 2.8 wt.% Fe, and (c) the steamed sample with 4.6 wt.% Fe.

be seen, the size distributions of the samples with 2.8, 4.6, and 6.7% Fe look very similar being the mean values calculated from the histograms 3.1, 3.7, and 3.5 nm, respectively.

To get information about the crystal structure of the particles, microdiffraction experiments were also performed. No crystalline patterns were observed, indicating a low crystallinity of the particles.

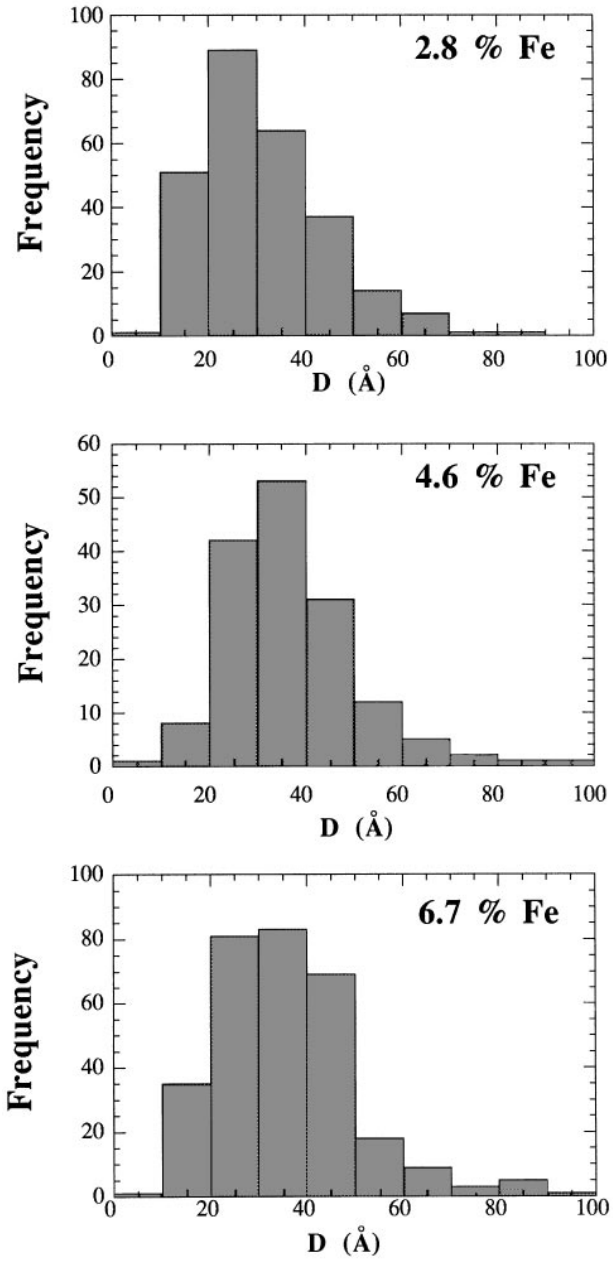

FIG. 2. Particle size histograms determined from the TEM micrographs of the steamed 2.8, 4.6, and 6.7 wt. % Fe samples.

B. Mössbauer spectroscopy

From previous Mössbauer experiments on this type of systems, it is known that the value of the isomer shift parameter δ provides atomic-scale information on the environment of the iron atoms.[8,15] As a rule of thumb, spectra with $\delta < 0.3$ mms^{-1} correspond to ions in tetrahedral coordination while spectra with $\delta > 0.3$ mms^{-1} indicate octahedral coordination. In as-synthesized ZSM-5-type ferrisilicates the Fe ions were found to be tetrahedrally coordinated, while in calcined or hydrothermally treated samples it was found to be octahedrally coordinated, and was tentatively attributed to extra-framework iron oxide.[8] Thus, the isomer shift criterion can be used to assist the identification of extra-framework states.

For our Mössbauer investigations we focused on as-synthesized and hydrothermally treated samples with an iron concentration of 4.6 wt. %. Spectra as recorded in zero field at room temperature and 4.2 K, and in an applied field of 10 T at 4.2 K, are shown in Figs. 3 and 4. All data were analyzed using a simple least-squares fitting program assuming Lorentzian lineshapes. Selected parameters from these fits are given in Table II.

1. As-synthesized sample

At room temperature and 4.2 K the zero field spectra show two components: a broad singlet and a narrow doublet. The persistence of the broad singlet at 4.2 K implies that it originates in paramagnetic relaxation; the onset of magnetic ordering visible in the wings of the singlet subspectrum at 4.2 K is consistent with this interpretation. The room temperature quadrupole splitting of the narrow doublet, 0.53 mms^{-1}, is smaller

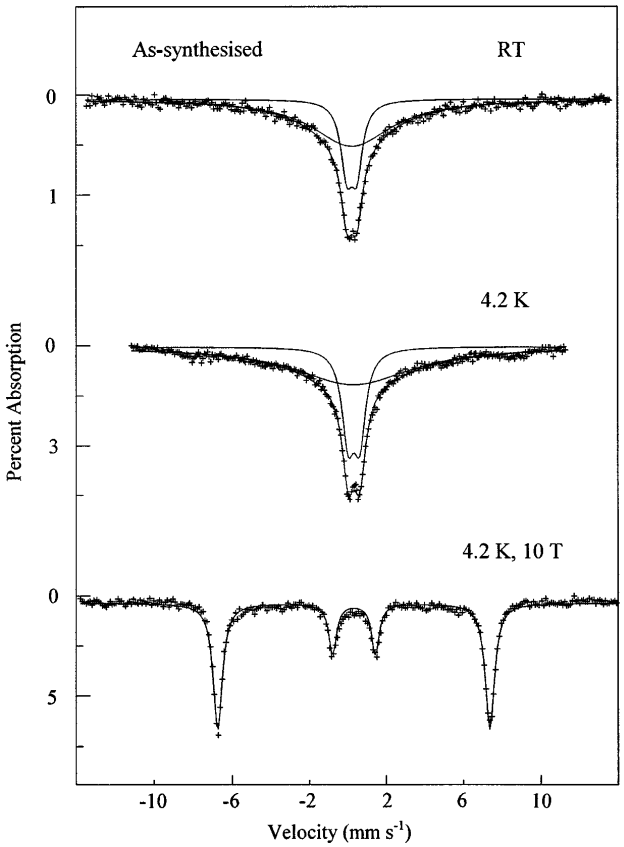

FIG. 3. Mössbauer spectra of the as-synthesized 4.6 wt. % Fe sample. In the figure the spectra at zero field, at room temperature, and 4.2 K, and the spectrum at 4.2 K with an applied field of 10 T are shown.

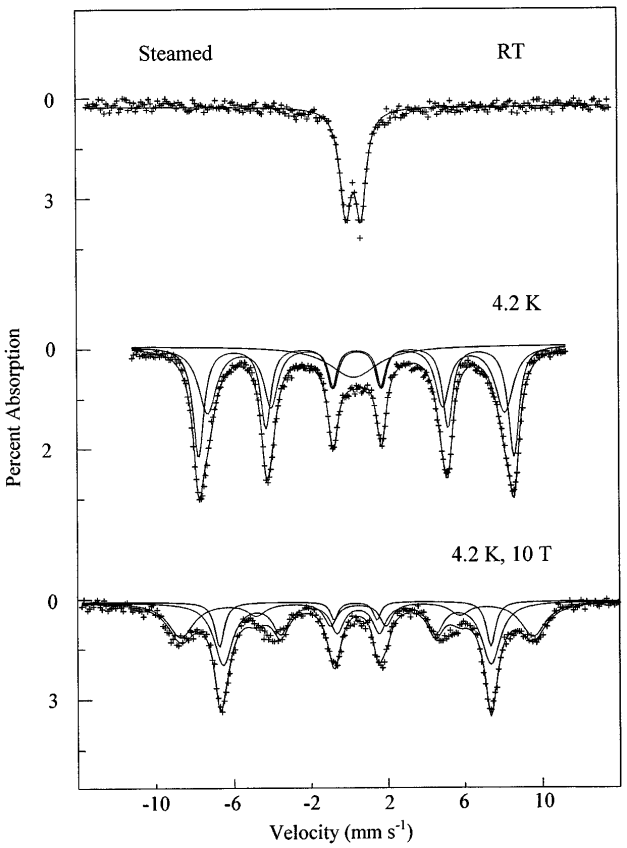

FIG. 4. Mössbauer spectra of the hydrothermally treated 4.6 wt. % Fe sample. In the figure the spectra at zero field, at room temperature, and 4.2 K, and the spectrum at 4.2 K with an applied field of 10 T are shown.

than the $\sim$0.65 mms^{-1} typically found in octahedrally coordinated Fe oxides. The isomer shift of both components at room temperature is $<$0.3 mms^{-1}, implying that the iron is in a tetrahedral coordination. In an applied field of 10 T parallel to the γ-ray beam at 4.2 K, four sharp lines appear. This spectrum is a magnetic hyperfine sextet, with line intensities in the ratio 3 : 0 : 1 : 1 : 0 : 3 in order of increasing Doppler velocity. The absence of lines two and five of the sextet shows that the Fe moments are collinear with the γ-ray beam, and therefore collinear with the applied field also. This is consistent with the response of a paramagnetic system to a large applied field.

The Mössbauer data for the as-synthesized sample lead to the conclusion that the iron ions are situated in the ferrisilicate framework, are tetrahedrally coordinated to framework oxygens, and are isolated from each other. This conclusion is consistent with the white color of the sample.

2. Hydrothermally treated sample

The room temperature spectrum is a sharp doublet. The isomer shift is $>$0.3 mms^{-1}, implying that the iron is octahedrally coordinated. A well-defined but broad sextet is found at 4.2 K, along with some remaining paramagnetic (or superparamagnetic) ions evidenced by a central absorption singlet. In an applied field of 10 T, the spectrum shows that at least two magnetic components are present. In the applied field spectrum the absorption lines in the outer wings, at approximately -9 and $+10$ mms^{-1} correspond to a component magnetic sextet with a relatively high effective field (see Table II), and can largely be attributed to the summation of the hyperfine field at the Fe nucleus and the 10 T applied field. Since the hyperfine field of a ferric ion is antiparallel to its atomic moment, this observation implies that some of the Fe moments in the material are (at least approximately) aligned antiparallel to the applied field. This suggests that the component has a ferrimagnetic character.

To test this suggestion we assumed that some of the Fe in the sample was still in the framework paramagnetic state. Since the overlap of lines in the 10 T spectrum made the fitting unreliable, we assumed that the relative area fraction of the paramagnetic component was the same as that seen for the central singlet component in the 4.2 K zero field spectrum. This fraction, $\sim$14%, was used to fit a constrained four-line paramagnetic subspectrum in the applied field spectrum, as shown in Fig. 4. In Fig. 5, this paramagnetic spectrum was subtracted to leave the ferrimagnet-like spectrum. Comparison with known patterns for iron oxides and oxy-

TABLE II. Selected parameters derived from least-squares fits of the Mössbauer data for as-synthesized and hydrothermally treated ferrisilicates containing 4.6 wt. % iron. The parameters are as follows. At room temperature: the isomer shift (δ) and the quadrupole splitting (QS). At 4.2 K in an applied field of 10 T: the fraction of the spectral area f_{pm} of the paramagnetic component, the effective hyperfine field B_{mag} of the para-, antiferro-, or ferrimagnetic component, and the relative area x of the second and fifth lines of the antiferro- or ferrimagnetic sextet, assuming an area ratio of 3 : x : 1 : 1 : x : 3 for the six lines. The number in the parentheses is the uncertainty on the last digit of each parameter.

Sample	δ (mms^{-1})	QS (mms^{-1})	f_{pm}	B_{mag} (T)	x
As-synthesized	0.24 (1)	0.53 (2)[a]	1	43.7 (1)	
Hydrothermally	0.33 (1)	0.79 (1)	0.14 (2)[b]	43.1 (1)	1.24 (5)
treated				56.6 (1)	0.79 (6)

[a]For doublet component only.
[b]This value determined from the zero field 4.2 K spectrum.

hydroxides showed that the most similar one belongs to two-line ferrihydrite, the least crystalline of the recognized forms of ferrihydrite.[16] A simulated Mössbauer spectrum for two-line ferrihydrite in an applied field of 10 T is shown in Fig. 5. It is clear on inspection that although the line positions of the two spectra are quite similar, the line intensities do not correlate very well.

We conclude that for the hydrothermally treated sample ~86% of the Fe ions migrate out of the ferrisilicate lattice and form a new magnetic species. This species is disordered and ferrimagnet-like, and resembles two-line ferrihydrite.

C. AC susceptibility

In this section the experimental χ_{ac} results are described. In what follows only data on representative samples will be shown in the figures, since the granulometric information, mostly based on the out-of-phase χ'' data, will be extensively analyzed in Sec. IV. To facilitate the understanding of these results, we also present in the Appendix a short analysis of the expected susceptibility of a mixture of noninteracting paramagnetic ions and superparamagnetic particles.

The in-phase susceptibility χ' of all the as-synthesized samples closely followed the Curie law (see Fig. 6 for data of a representative sample). This fact, and the negligible out-of-phase susceptibility χ'' in the whole temperature range, are the characteristics of a paramagnet. The effective moments obtained from the Curie law range between 5.0 and 6.5 μ_B with an estimated error of ~10%, mainly due to the error in the determination of the iron content in the samples. Within this accuracy, these values are close to 5.9 μ_B, which is the typical value for Fe(III) in tetrahedral environment.[17] The as-synthesized 6.7 wt. % Fe sample exhibits a sizeable rise in χ'' (data not shown) at the lowest temperatures, although, following the rule for the lower concentrations, no peak is observed in $\chi'(T)$. This rise in χ'' may be due to the formation of very small particles, and it would indicate that above a certain iron concentration the iron ions cannot be incorporated in the framework even in the as-synthesized state.

The steamed samples behaved as follows. For the 0.5 wt. % Fe sample, the ac susceptibility coincides with that of a paramagnet (Fig. 7). The temperature dependence of the in-phase susceptibility gives an effective moment per iron ion of 4.6 μ_B. In the figure, it can be seen that the reciprocal of χ' is slightly bent upward in the high temperature range. This effect is due to the diamagnetic contribution of the matrix, and its is particularly visible in this sample because, due to its low

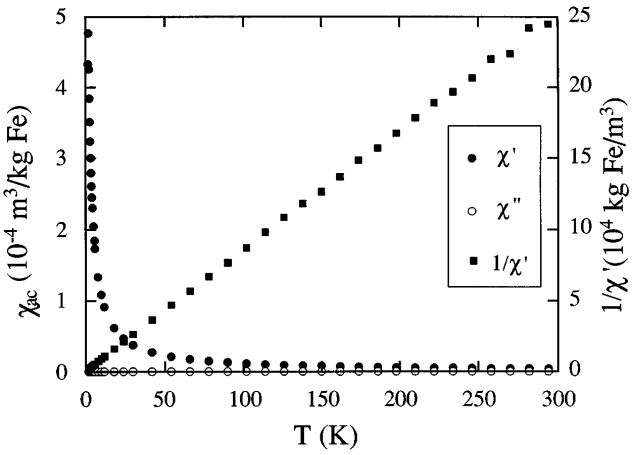

FIG. 6. Temperature dependence of the in-phase ac susceptibility at 0.1 Hz of the as-synthesized 4.6 wt. % Fe sample together with the reciprocal of the in-phase component.

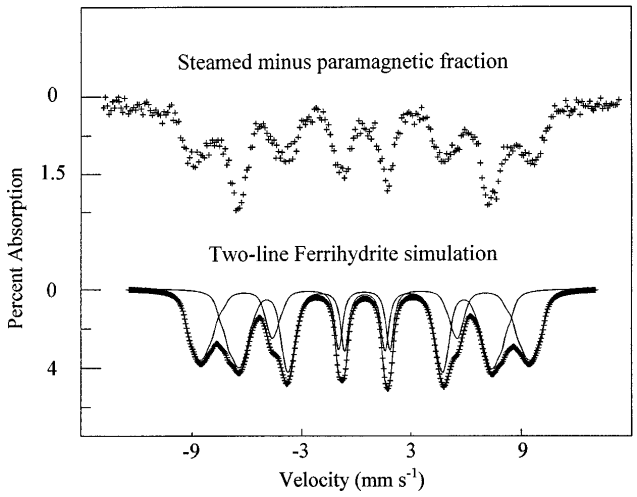

FIG. 5. Comparison of the experimental Mössbauer spectrum of the steamed 4.6 wt. % Fe sample, after subtraction of the paramagnetic component, with a simulated spectrum for two-line ferrihydrite.

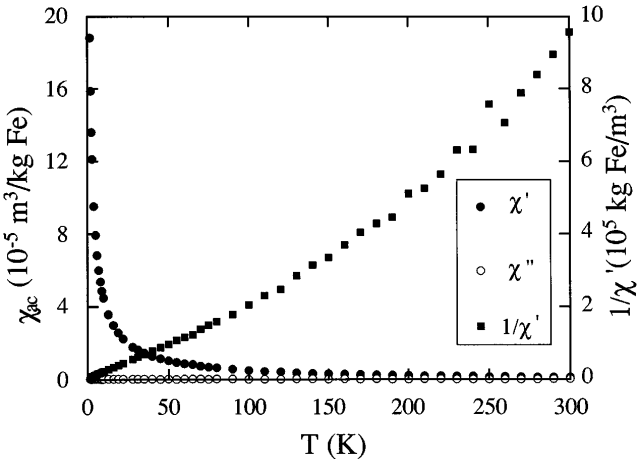

FIG. 7. Temperature dependence of the in-phase and out-of-phase ac susceptibility at 119 Hz of the hydrothermally treated 0.5 wt. % Fe sample together with the reciprocal of the in-phase component. The slight bending of $1/\chi'$ is due to diamagnetic contributions (see text).

iron concentration, its relative contribution is the highest compared with the iron paramagnetism. χ'' remains negligible in the whole temperature range, indicating the absence of relaxing entities.

The in-phase susceptibility of the steamed sample with 1.0 wt.% Fe also followed a Curie law over the full temperature range (data not shown). Nevertheless, the effective moment per iron ion results in 8.7 μ_B. This fact, together with the small maximum observed in χ'' at low temperatures, indicates the presence of some very small particles starting to experience relaxation at those temperatures.

At high temperatures, the steamed samples with 1.5, 2.8, and 4.6 wt.% Fe all showed Curie law behavior (see Fig. 8 for data on a representative sample). The presence of an assembly of small magnetic particles was evidenced by a blocking maximum in χ' at around 13 K, accompanied by a maximum in χ'' at slightly lower temperatures, and by the large effective moments determined from the Curie law: 17.0, 15.2, and 14.1 μ_B, respectively. At low temperatures there is a $\chi'(T)$ rise which has no counterpart in $\chi''(T)$. This phenomenon, which has no relaxational character, is paramagnetic-like, and is caused by the presence of entities with very low anisotropy energy, in particular the still isolated framework iron ions.

The steamed sample with 6.7 wt.% Fe showed the same behavior as the previous ones except for additional anomalies in χ' and χ'' at about 100 K, suggesting the existence of a small fraction of large particles (data not shown).

D. Field dependent magnetization

The magnetization as a function of applied field of the measured as-synthesized samples follows a straight line (data not shown), as expected for Brillouin paramagnetism at low fields, up to the highest available field (5 T).

The magnetization curves of the steamed samples are shown in Fig. 9. For the lowest iron content (0.4 wt.%) the magnetization closely follows that of a paramagnet, and up to 5 T, $M(H)$ is linear. The $M(H)$ curves of samples with 1.6, 2.8, 4.6, and 6.7 wt.% Fe look very similar. The magnetization of the sample with 1.0 wt.% Fe presents an intermediate behavior.

The magnetization curve of a system of noninteracting small magnetic particles can be fitted to a distribution of Langevin functions only if the thermal energy is much larger than the single particle anisotropy energy.[18] For this reason, as well as to get rid of remanences which did appear at lower temperatures, we have performed the $M(H)$ measurements at the highest available temperature (290 K). We have attempted to fit the $M(H)$ curves to sums of Langevin

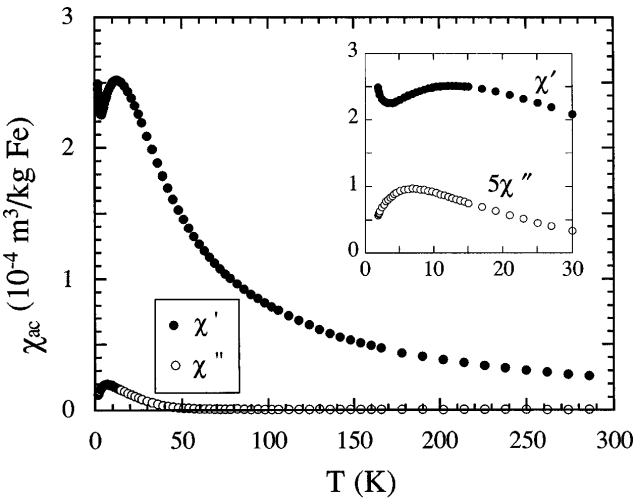

FIG. 8. Temperature dependence of the ac susceptibility at 119 Hz of the hydrothermally treated 1.6 wt.% Fe sample. In the inset it is shown the temperature region where substantial magnetic relaxation takes place. The small tail at low temperature, which has no counterpart in $\chi''(T)$, is indicative of residual paramagnetism.

functions. However, since in all cases the magnetization at 5 T is far from saturation, it is impossible to rigorously determine the saturation magnetization, a necessary parameter for such calculation. The comparison between the magnetization curves for the different concentrations will inform us though about the magnetic character of the particles, as will be discussed in the next section.

IV. DISCUSSION

Before analyzing the effects produced by the hydrothermal treatments, we have shown that the starting, nonsteamed, ferrisilicates with iron contents between 0.4 and 4.6 wt.% behave as paramagnets due to their isolated Fe(III) ions.

The actual nature of the particles generated in the steamed samples is difficult to determine. The Mössbauer results pointing to two-line ferrihydrite agree with the microdiffraction experiments in that the particles present a low crystallinity. In spite of its intrinsic disorder, the published data for ferrihydrite indicate a trigonal unit cell with $a = 0.508$ nm and $c = 0.94$ nm.[19] Consequently, following the comment made in the introduction in the paper, strong difficulties appear in their identification, as they are entities with size of the order of the lattice parameter.

However, some information on the magnetic order of the particles can be obtained from the magnetization curves. If one assumes isolated iron ions, the magnetization will scale with the iron concentration and, as a function of applied field, will follow a unique paramagnetic Brillouin curve. If a fraction of the magnetic ions are present as antiferromagnetic particles, the

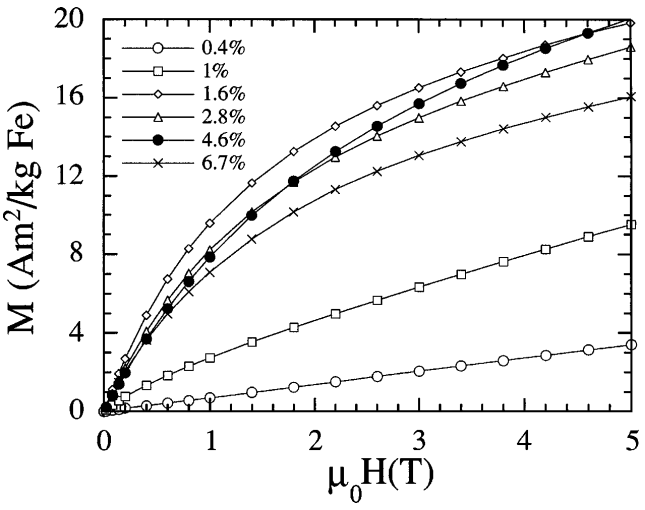

FIG. 9. Magnetization, expressed in relative units with respect to the iron amount, as a function of applied field, at 290 K for the hydrothermally treated samples. The accuracy of the magnetization values is limited, like the effective moments obtained from susceptibility (see text), by the error in the determination of the iron amount in each sample.

magnetization curve $M(H)$ exhibits approximately (see Appendix) the same initial slope (initial susceptibility), but deviates downward with respect to the paramagnetic curve.[20] As can be seen our $M(H)$ curves lie *above* the paramagnetic one (see Fig. 9), indicating that at least a fraction of particles present a ferro- or ferrimagnetic character.

As we are going to deal with the magnetic behavior of an assembly of magnetic particles, it is pertinent to estimate the importance of dipole-dipole interactions in order to make a reliable interpretation of the data. It is customary to define the quantity $T_{\mathrm{dip}} = (\mu_0/4\pi)(m^2/k_B a^3)$, where a is a measure of the distance between pairs of dipole moments, m the magnetic dipole moment, and k_B the Boltzmann constant. Since a good estimate for a is $N^{-1/3}$, being N the number of dipoles per unit volume, it results $T_{\mathrm{dip}} = (\mu_0/4\pi)(Nm^2/k_B)$. This value is proportional to the Curie constant; therefore its calculation from the Curie law susceptibility is straightforward and circumvents any knowledge of the interdistance or the moment of the particles. In our case we obtain $T_{\mathrm{dip}} = 0.21$ K for the most concentrated sample, which is substantially lower than the temperatures in which the magnetic relaxation anomalies take place, making it reasonable the use of the noninteraction approximation.

In addition to the TEM characterization, we shall analyze the $\chi_{\mathrm{ac}}(T)$ data to obtain complementary information on the particle size distribution. Generally a relaxation time is associated to any magnetic particle in order to represent the probability of its magnetic moment for jumping over its anisotropy energy barrier. Although the activation energy E of this process depends on many factors, including surface and shape effects, we shall make the customary assumption $E = KV$, where K is an effective anisotropy constant and V is the particle volume. The complex susceptibility of an assembly of noninteracting particles can be obtained by summing over the distribution of activation energies. In this way, both the in-phase and the out-of-phase components can be expressed as a function of the distribution. In our case we have made use of the expression for the out-of-phase component

$$\chi''(T) = \frac{\pi}{6}\,\mu_0\left(\frac{M_s^2 x_P}{3K\tilde{\rho}}\right) D f(D), \qquad (1)$$

which has been derived under the assumptions of Debye relaxation and Arrhenius temperature dependence of the relaxation times.[21] In this expression, χ is the susceptibility per iron mass in the sample, x_P is the fraction of iron mass present in particles, $\tilde{\rho}$ is the iron mass per unit volume in the particles,[22] M_s is the spontaneous magnetization of the particles, D is the diameter of a particle that becomes blocked at temperature T, which is expressed by

$$D = \left[\frac{6k_B T}{\pi K}\,\ln\left(\frac{\nu_0}{\omega}\right)\right]^{1/3}, \qquad (2)$$

where ν_0 is a preexponential factor and $\omega/2\pi$ is the measuring frequency, and $f(D)\,dD$ is the normalized volume fraction occupied by particles with diameters between D and $D + dD$. Following these expressions, if ν_0 and K are known parameters, the particle size distribution can easily be obtained from the $\chi''(T)$ data.

Equation (1) implies that, for a given particle size distribution, the experimental $\chi''(T,\omega)$ data, expressed as a function of the variable $k_B T \ln(\nu_0/\omega)$, must collapse into a master curve. Hence, the search for optimum collapsing of χ'' data allows one to determine the preexponential factor ν_0. This method, unlike other ones based on χ' data, is particularly useful for our systems since it is independent of the presence of nonrelaxing entities, in particular of paramagnetic character. For this purpose, our samples have been analyzed in the frequency range 0.1–120 Hz, yielding by this procedure a preexponential factor $\nu_0 = 10^{13\pm0.5}$ Hz.

From Eq. (1) it also follows that the function $f(D)$ is proportional to the function $\chi''(T)/D$. If the former is calculated after the size distributions determined by TEM, and the latter from the experimental susceptibility data, it is possible, by means of Eq. (2), to determine the effective anisotropy constant K. In our case the data obtained from TEM and χ'' have been fitted to gamma distribution functions whose identification allows to calculate K. The value obtained has been $K = 2.2 \pm 0.2 \times 10^4$ J/m^3, using the data for the sample with 2.8% Fe

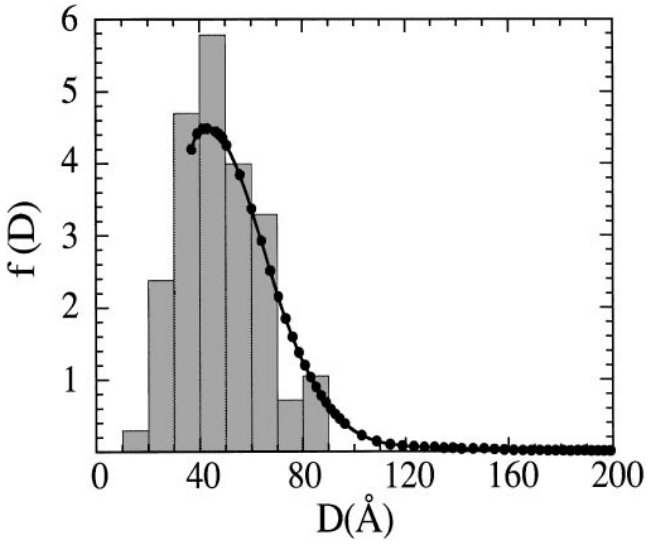

FIG. 10. Identification of the particle size distribution obtained from the TEM and $\chi''(T)$ for the steamed sample of 2.8% Fe in order to determine the effective anisotropy constant K.

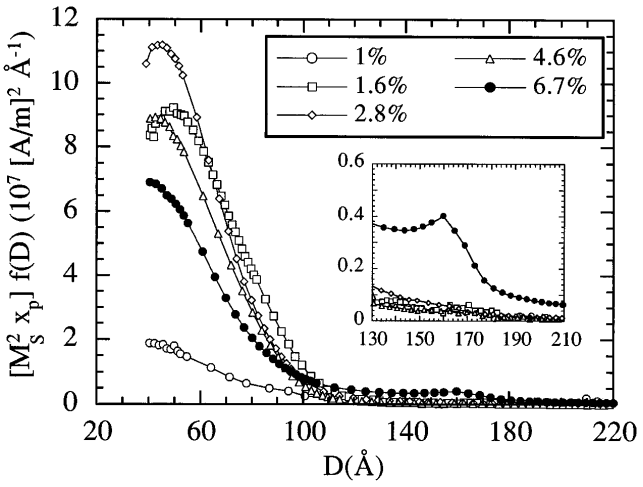

FIG. 11. Particle size distributions obtained from the $\chi''(T)$ analysis. In the vertical axis the distribution function $f(D)$ multiplied by x_P and M_s^2, as it is directly obtained from Eq. (1), is represented. If the same M_s is assumed for the particles in all the samples, the higher the curves the higher the iron fraction x_p in particles. In particular, in the low iron content 1% Fe sample, there is little chance for the iron ions to aggregate into particles of detectable size. It is shown in the inset that the 6.7% Fe sample apparently contains a fraction of large particles, although in a small amount, whose effect is also visible in the small $\chi(T)$ anomaly around 100 K mentioned in the text.

(identification shown in Fig. 10). From the very similar TEM results and since the same synthesis procedures have been used for the whole series of steamed samples, we find it reasonable to assume that the particles that they contain have same nature, hence we have treated all the χ'' data in the same way, viz., with the same K. This assumption, or, if it is possible in practice, any other determination of the anisotropy constant, confers to the χ'' treatment the ability of comparing particle size distributions among the studied samples. This type of *relative* granulometry is independent of the TEM results, as it is based on different phenomena, and, unlike the microscopical observations, informs simultaneously about the whole sample.

The so-obtained size distributions are presented in Fig. 11. In the steamed samples, the increase in iron concentration leads also to an increase in the number of particles per unit volume, while the size distribution itself seems not to be very much affected. Within the experimental error, this fact is also consistent with the TEM observations.

V. CONCLUSIONS

All the studied ferrisilicates in the as-synthesized state possess isolated Fe(III) ions in framework sites. Only for the highest iron concentration (6.7 wt.%) a small fraction of the iron may be in a clustered nonframework state.

The effects of migration of iron atoms from the framework under hydrothermal treatment have been studied. A substantial fraction of iron is involved in the formation of nanosize particles whose composition is presumably two-line-ferrihydrite, the remainder being still smaller species that might include isolated in-framework iron ions and very small iron-containing clusters. The particles formed are superparamagnetic at high temperature and become magnetically blocked around 15 K due to their magnetic anisotropy.

$\chi_{ac}(T)$ and $M(H)$ data indicate that the intraparticle magnetic ordering cannot be antiferromagnetic, at least if a spin uncompensation based on the random walk model ($m \propto \mu n^{1/2}$), as proposed by Néel, is considered. Instead, from Mössbauer, $\chi(T)$ and $M(T)$ data, it is concluded that it originates on intrinsic ferrimagnetism. The effective anisotropy constant resulting from a combined use of TEM and ac susceptibility is $2.2 \pm 0.2 \times 10^4$ J/m^3.

From several granulometric methods which make use of TEM, $M(H)$, $\chi_{ac}(T)$ data, it has been observed that for the lowest iron concentration the hydrothermally treated sample is still a paramagnet; however, above 1.5% Fe there is an increasing amount of small particles whose size distribution is apparently independent on the iron content. The TEM analysis shows that the particles are dispersed in the ferrisilicate crystallites and do not present aggregation.

With a suitable election of the magnetically active element and the structure of the molecular sieve, the system studied in this work may offer new possibilities for the production of nonaggregated small particle assemblies, of potential use as model systems in nanoparticle magnetism research.

ACKNOWLEDGMENTS

This work has been financed by Diputación General de Aragón (DGA) under Project No. PIT0892 and by Fundación Ramón Areces. The authors are grateful to F. Luis for many fruitful discussions, J. L. G-P. Thanks CONSI + D (DGA) for a grant (BIT 1292).

REFERENCES

1. R. W. Siegel, Nanostructured Mater. **3**, 1 (1993).
2. S. W. Charles and J. Popplewell, in *Ferromagnetic Materials*, edited by E. P. Wohlfarth (North Holland, Amsterdam, 1980), Vol. II.
3. T. Bitoh, K. Ohba, M. Takamatsu, T. Shirane, and S. Chikazawa, J. Phys. Soc. Jpn. **62**, 2583 (1993); C. L. Chien, Annu. Rev. Mater. Sci. **25**, 129 (1995).
4. J. W. Nemantsverdriet, in *Magnetic Properties of Fine Particles*, edited by J. L. Dormann and D. Fiorani (Elsevier, Amsterdam, 1992).
5. R. D. Shull, Nanostructured Mater. **2**, 213 (1993).
6. S. Kawi and B. C. Gates, in *Clusters and Colloids, From Theory to Applications*, edited by G. Schmid (VCH, Weinheim, Germany, 1994).
7. H. Topsøe, J. A. Dumesic, and S. Mørup, in *Applications of Mössbauer Spectroscopy*, edited by R. L. Cohen (Academic Press, New York, 1980), Vol. II.
8. A. Meagher, V. Nair, and R. Szostak, Zeolites **8**, 3 (1988).
9. R. T. Obermyer, L. N. Mulay, C. Lo, M. Oskooie-Tabrizi, and V. U. S. Rao, J. Appl. Phys. **53**, 2683 (1982).
10. J. L. García, F. J. Lázaro, C. Martínez, and A. Corma, J. Magn. Magn. Mater. **140–144**, 363 (1995); J. L. García, A. López, F. J. Lázaro, C. Martínez, and A. Corma, J. Magn. Magn. Mater. **157–158**, 272 (1996).
11. F. J. Lázaro, J. L. García, V. Schünemann, Ch. Butzlaff, A. Larrea, and M. A. Załuska-Kotur, Phys. Rev. B **53**, 13 934 (1996).
12. R. Szostak, *Molecular Sieves, Principles of Synthesis and Identification* (Van Nostrand Reinhold, New York, 1989).
13. MFI is the name of the structure type, to which our ferrisilicates and the ZSM-5 zeolite are isomorphous. This structure contains pores of around 5.6 Å in diameter. For details see W. M. Meier and D. H. Olson, *Atlas of Zeolite Structure Types* (Butterworth-Heinemann, 1992).
14. R. J. Argauer and G. R. Landolt, U.S. Patent 3 702 886 (1972).
15. R. L. Garten, W. N. Delgass, and M. Boudart, J. Catal. **18**, 90 (1970).
16. Q. A. Pankhurst, Hyperfine Interactions **90**, 201 (1994).
17. A. Abragam and B. Bleaney, *Electron Paramagnetic Resonance of Transition Ions* (Oxford University Press, 1970).
18. H. D. Williams, K. O'Grady, M. El Hilo, and R. W. Chantrell, J. Magn. Magn. Mater. **122**, 129 (1993).
19. C. W. Childs, Z. Pflanzenernähr. Bodenk. **154**, 441 (1992).
20. If the intraparticle negative spin correlations are maintained, the saturation magnetization of the assembly, due only to spin uncompensations, is obviously smaller than in a paramagnet.
21. M. I. Shliomis and V. I. Stepanov, in *Relaxation Phenomena in Condensed Matter*, edited by W. Coffey, Advances in Chemical Physics Series, Vol. LXXXVII (John Wiley and Sons, 1994), p. 1. In the original paper, an extra factor $\pi/18$ is apparently absent. Due to our low measuring frequencies, the parameter $S(\sigma)$ appearing in the original paper has been taken as unity.
22. Although the nature of the particles is not completely known, in this work we used $\tilde{\rho} = 2494$ kgFe/m^3 as it has been determined for ferrihydrite in J. M. D. Coey, J. Phys. Cond. Matter. **5**, 7297 (1993).
23. L. Néel, J. Phys. Soc. Jpn. **17**, supp. B-I, 676 (1962). See also Q. A. Pankhurst and R. J. Pollard, J. Phys. Cond. Matter. **5**, 8487 (1993), and references therein.
24. See, for example, J. L. Dormann, Revue Phys. Appl. **16**, 275 (1981), and references therein.

APPENDIX

Both para- and superparamagnetic systems are, by definition, assemblies of noninteracting magnetic entities. For static measuring fields, the temperature dependence of their initial (zero field limit) susceptibility follows the Curie law

$$\chi = \frac{\mu_0 N m^2}{3k_B T}, \tag{A1}$$

where N is the number of entities per unit volume, each one carrying a magnetic moment m, and k_B is the Boltzmann constant. In the case of paramagnets m equals the single ion magnetic moment μ. In the case of superparamagnets, m represents the total magnetic moment of the particle which, depending on its size and internal magnetic ordering, may be some orders of magnitude greater than μ. In dynamic measurements (ac susceptibility), when a zero out-of-phase χ'' component is observed, the in-phase component χ' equals the static susceptibility. If, in addition, the ac measuring field is low, the χ' observed in these systems approaches the initial susceptibility and can be interpreted in terms of the Curie law.

In real materials, when magnetically active ions are included in the synthesis and there is a chance for them to aggregate in some way to form small magnetic particles, the amount of magnetic ions per unit mass (or volume) is determined from the preparation conditions, while the number (alternatively the magnetic moment) of the particles is generally unknown. In spite of this, it is possible to retrieve some information from the susceptibility data by the following procedure. If the sample contains magnetic particles with a distribution of magnetic moments, the total susceptibility is

$$\chi = \frac{\mu_0}{3k_B T} \sum n_i m_i^2, \tag{A2}$$

where n_i is the number of entities per unit volume, each one carrying a moment m_i. Nevertheless, if the experimental susceptibility is forced to follow Eq. (A1), taking as a value for N, the *known* number of ions per unit volume, we can define an effective moment per ion

$$m_{\text{eff}} = \left(\frac{\sum n_i m_i^2}{N} \right)^{1/2}. \tag{A3}$$

In the case of an assembly of N_p particles per unit volume, all identical, with n spins per particle, $N =$

$N_p n$. If, moreover, the particles are ferromagnetic and $m_i = n\mu$ is a good representation of their type of magnetism, the effective moment becomes

$$m_{\text{eff}} = \left(\frac{N_p \mu^2 n^2}{N}\right)^{1/2} = \mu\sqrt{n}\,. \qquad \text{(A4)}$$

In the particular case of a paramagnet, $m_i = \mu$ and $\Sigma n_i = N$; hence m_{eff} equals μ. However, if all or a part of the entities are ferromagnetic particles, the effective moment per ion results *higher* than the single ion value.

An interesting case are the antiferromagnetic particles. In the ideal case, a fully ordered anitferromagnetic particle will carry zero magnetic comment. Nevertheless it is observed in practice that they do possess a net magnetic moment due to spin uncompensation. It has been proposed by Néel that this net moment is proportional to the square root of the number of spins in the particle, although the proportionality constant may depend on the type of lattice.[23] Therefore, if one assumes a magnetic moment per particle $\gamma\mu n^{1/2}$, where γ is a constant rather close to unity for an intraparticle three-dimensional array of spins,

$$m_{\text{eff}} = \left(\frac{N_p \gamma^2 \mu^2 n}{N}\right)^{1/2} = \gamma\mu \approx \mu\,. \qquad \text{(A5)}$$

This expression implies that an assembly of antiferromagnetic particles has approximately the *same* effective moment per spin as a paramagnet. After these considerations it follows that an effective moment *higher* than the expected for a single ion indicates that at least a fraction of the entities contained in the material must have ferri- or ferromagnetic intraparticle ordering. Moreover, the additive character of the susceptibility allows one to extend this conclusion to mixtures of non interacting particles and paramagnetic ions.

From the point of view of dynamics, the validity of the Curie law is restricted to the case of magnetic moments reacting immediately to the application of the measuring field; nevertheless in magnetic particles their magnetic moments must surmount their anisotropy energy barrier. At sufficiently low temperatures, which depend on the particle size and on the measuring frequency, this fact leads to magnetic relaxation and is manifested by a departure of χ' from the Curie law accompanied by a nonzero χ''.[24]